Photocatalytic degradation of organic compounds by 2-ethylimidazole-treated titania under visible light illumination

Jiwon Seo[1,2], Junyoung Jeong[2] and Changha Lee[*1]

[1]*School of Chemical and Biological Engineering, Institute of Engineering Research, Seoul National University,*
[1]*Gwanak-ro, Gwanak-gu, Seoul 08826, Republic of Korea*
[2]*School of Urban and Environmental Engineering, Ulsan National Institute of Science and Technology (UNIST),*
50 UNIST-gil, Ulju-gun, Ulsan 44919, Republic of Korea

Abstract. Titania modified by 2-ethylimidazole (2-EI) (denoted as 2-EI-TiO$_2$) demonstrated visible light photocatalytic activity for the degradation of organic compounds. 2-EI-TiO$_2$ was a bright brown powder that exhibited similar crystallinity and morphology with the control TiO$_2$. A diffuse reflectance spectrum indicated that 2-EI-TiO$_2$ absorbs visible light of all wavelengths. X-ray photoelectron spectroscopy (XPS) confirmed the cationic state of nitrogen species (e.g. Ti-O-N) on the surface of 2-EI-TiO$_2$. Visible light-illuminated 2-EI-TiO$_2$ degraded 10 μM 4-chlorophenol (4-CP) by approximately 85% in 4 h. The photochemical activity of 2-EI-TiO$_2$ was selective in targeting the organic compound. The repeated use of 2-EI-TiO$_2$ decreased the photocatalytic activity for the 4-CP degradation. Experiments using radical scavengers and oxidant probes revealed that the oxidation by photogenerated holes is responsible for the degradation of organic compounds by illuminated 2-EI-TiO$_2$ and the role of $^\bullet$OH is negligible.

Keywords: visible light; photocatalysis; titanium dioxide; 2-ethylimidazole; oxidation

1. Introduction

Titania (TiO$_2$) has been studied as a photocatalyst for the degradation of organic compounds because of its cost-efficiency, non–toxicity, photochemical–stability, and strong oxidizing power (Hoffmann *et al*. 1995, Fujishima *et al*. 2000). However, the photochemical reactions of TiO$_2$ usually require UV light due to the wide bandgap (approximately 3.2 eV and 3.0 eV for anatase and rutile, respectively), which limits their application (Vinu and Madras 2008). To extend the range of wavelengths available for TiO$_2$ photocatalysis, various approaches for surface modification have been attempted. Among those widely reported are the surface doping by metals and nonmetals.

Metal and nonmetal dopants generate mid-gap states between the valence band (VB) and the conduction band (CB) of TiO$_2$. Transition metals (Fe, Cu, Co, Ni, etc.) and noble metals (Pt, Au, Ag, etc.) have been typically used as metal dopants (Park *et al*. 2013, Schneider *et al*. 2014, Yuan *et al*. 2018). Metal-doping adjusts the bandgap of TiO$_2$ and promotes the interfacial electron transfer (Kim *et al*. 2005). However, some metal dopants can act as recombination sites of electron-hole pairs, inhibiting the generation of reactive species on the TiO$_2$ surface (Kang 2005, Pelaez *et al*. 2012).

Meanwhile, nonmetal-doping uses a different modification approach in which oxygen in the TiO$_2$ lattice is replaced by the doping element (C, F, S, etc.) (Yu *et al*. 2005, In *et al*. 2007, Periyat *et al*. 2008, Selvam and Swaminathan 2012, Neville *et al*. 2013, Wang *et al*. 2017). Among the nonmetal dopants, nitrogen is considered the most effective. Nitrogen can easily substitute in the TiO$_2$ lattice for oxygen because of its small ionization energy, high stability, and atomic size that is comparable to oxygen (Pelaez *et al*. 2012). Several investigators have examined the visible light activity of nitrogen-doped TiO$_2$ to degrade organic compounds (Gole *et al*. 2004, Sathish *et al*. 2007, He *et al*. 2014).

In this study, a new nitrogen-doped TiO$_2$ photocatalyst was synthesized by a simple modification of commercial TiO$_2$ using 2-ethylimidazole (2-EI) as a nitrogen-doping agent (denoted as 2-EI-TiO$_2$). The synthesized material was characterized by various analytical tools. In addition, 2-EI-TiO$_2$ was examined for its photocatalytic activity to degrade different organic compounds under visible light illumination. Then the photocatalytic activity of 2-EI-TiO$_2$ was compared to that of bare TiO$_2$. The photochemical stability of 2-EI-TiO$_2$ was also examined by repetition tests. Lastly, the mechanism of degrading the organic compound by the illuminated 2-EI-TiO$_2$ is discussed.

2. Materials and methods

2.1 Reagents

All chemicals were of reagent grade and used without further purification except for 2,4-dinitrophenyl hydrazine (DNPH). DNPH was recrystallized three times using

---

∗Corresponding author, Professor
 E-mail: leechangha@snu.ac.kr

acetonitrile. Chemicals used in this study included TiO₂ (P25, Degussa Co.), 2-ethylimidazole (2-EI), perchloric acid, sodium hydroxide, benzoic acid (BA), phenol, 4-chlorophenol (4-CP), acetaminophen (AAP), carbamazepine (CBZ), *para*-hydrobenzoic acid (*p*-HBA), formaldehyde (HCHO), methanol, *tert*-butanol, DNPH, phosphoric acid (all from Sigma-Aldrich Co.), microcystin-LR (MC-LR, Enzo Life Science Inc.), and acetonitrile (J.T. Baker Co.). Stock solutions were prepared for phenol (10 mM), 4-CP (10 mM), BA (10 mM), AAP (1 mM), CBZ (0.1 mM), *p*-HBA (10 mM), and MC-LR (0.5 mM). The stock solutions were prepared in deionized (DI) water (18.2 MΩ Milli-Q water, Millipore Co.) and stored at 4°C until use.

2.2 Synthesis of 2-EI-TiO₂

2-EI (1.6 g) was dissolved in DI water (10 mL), and subsequently P25 (0.2 g) was suspended in the solution. Then, the suspension was dried at 50°C while stirring until a white powder was obtained. The powder was sintered at 350°C in a muffle furnace for 3 h under N₂ condition. Finally, the material was washed with DI water to remove residual impurities and dried at 50°C.

2.3 Characterization

Transmission electron microscopy (TEM) (JEM-2100, Jeol Co.) was used to characterize the morphology of the materials. X-ray diffraction patterns of materials were recorded by an X-ray diffractometer (D8 Advance, Bruker AXS Inc.) with Cu-Kα radiation. Diffuse reflectance spectra were obtained using a UV/Vis/Near IR spectrophotometer (Cary 5000, Agilent Co.). X-ray photoelectron spectroscopy (XPS) with Al-Kα radiation (K-alpha, Thermo Fisher Scientific Inc.) was used to analyze surface elemental distributions of materials.

2.4 Experimental setup and procedure

All experiments were performed in a cylindrical quartz batch reactor at room temperature (22 ± 2°C). The experiments regarding photocatalytic degradation of organic compounds except for MC-LR were performed using fluorescent lamps (six 4 W lamps, Shin-Kwang Electronics Co.) with a 400 nm longpass filter in a dark chamber. The experiments using MC-LR and oxidant probes were performed by a 150 W xenon arc lamp system (LS 150, Abet Technologies Inc.) equipped with both an AM 1.5G filter and a 400 nm longpass filter.

The reaction solution (50 mL) was prepared by adding the photocatalyst powder (0.5 g/L) and the target compound (10 μM). The initial pH of the solution was adjusted to 5.0, except for the MC-LR experiment where the initial pH of the solution was adjusted to 7.0. The photochemical reaction was initiated by light illumination. Samples were taken at predetermined time intervals, and immediately filtered using a 0.45 μm PTFE syringe filter (Advantech Co.).

2.5 Analytical methods

The concentrations of organic compounds were measured by high performance liquid chromatography (HPLC, UltiMate™ 3000, Thermo Fisher Scientific Inc.) with UV absorbance detection at 230, 227, 277, 241, 285, 350, 270, and 238 nm for 4-CP, BA, phenol, AAP, CBZ, HCHO, *p*-HBA, and MC-LR, respectively. The chromatographic separation was performed on a ZORBAX Eclipse XDB-C18 column (150 mm × 4.6 mm, 5 μm, Agilent Co.) using 50:50–90:10 mixtures of 0.1% phosphoric acid solution and acetonitrile as the eluent at a flow rate of 1.5 mL/min. For the separation of MC-LR, an Acclaim™ C18 column (150 mm × 2.1 mm, 2.2 μm, Thermo Fisher Scientific Inc.) was used with flowing a 65:35 mixture of 0.05% trifluoroacetic acid (TFA) solution and methanol at 0.5 mL/min.

3. Results

3.1 Synthesis and characterization of 2-EI-TiO₂

Different materials of 2-EI-TiO₂ were synthesized with varying the sintering temperature, and these materials were tested for the 4-CP degradation under visible light illumination (Fig. 1). The photographs of the materials show that 2-EI-TiO₂ synthesized at a low sintering temperature (250°C) is dark-brown. The color of 2-EI-TiO₂ fades out with increasing the sintering temperature (Fig. 1(a)). The materials synthesized at >400°C were almost white, undistinguishable from the bare TiO₂.

The materials synthesized at 350°C exhibited the highest photocatalytic activity to degrade 4-CP (Fig. 1(b)) The pseudo-first order rate constant for the degradation of 4-CP by 2-EI-TiO₂ increased with increased sintering temperature from 250°C to 350°C, but it drastically dropped after 400°C (Fig. 1(b)). Therefore, the 2-EI-TiO₂ material synthesized at 350°C was used for further experiments.

The crystallinity of 2-EI-TiO₂ and bare TiO₂ were investigated by XRD techniques. The XRD patterns of both materials showed similar signals of mixed anatase and rutile phases (Fig. 2(a)). It is known that the metastable anatase phase can be irreversibly transformed into stable rutile phase at elevated temperatures (Hanaor and Sorrell 2011). However, these phase transition starts at approximately 600 to 700°C, and thereby it appears that the sintering process of 2-EI-TiO₂ does not lead to the phase transition. TEM images of 2-EI-TiO₂ and bare TiO₂ also show that both materials consist of similar rectangular nanoparticles of 20-30 nm in size (Fig. 2(b)).

The 2-EI-TiO₂ material is bright brown powder, which indicates visible light absorption. The diffuse reflectance spectra show that 2-EI-TiO₂ exhibits enhanced light absorption in the entire wavelength range of 350 to 800 nm compared to the bare TiO₂ (Fig. 2(c)). To determine the bandgap of 2-EI-TiO₂ and bare TiO₂, a plot of modified Kubelka-Munk function versus the light energy was used (Sakthivel and Kisch 2003, Devi *et al.* 2012, Ruqaishy *et al.* 2018). The Kubelka-Munk function (F(R)) is expressed as equation (1), where R is the relative reflectance ratio of sample to standard BaSO₄.
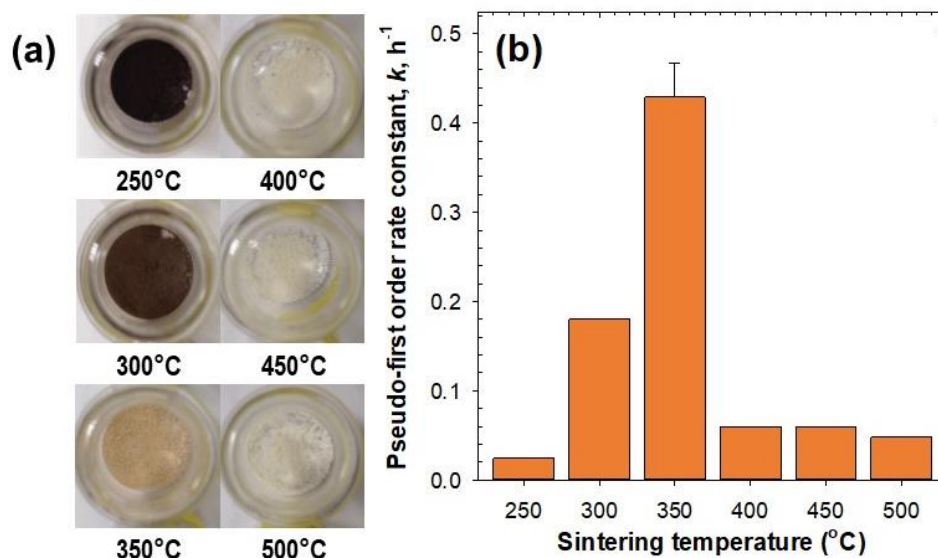
$$F(R) = \frac{(1 - R)^2}{2R} \qquad (1)$$

Fig. 1. Photographs of 2-EI-TiO$_2$ materials synthesized at different sintering temperatures (a), and pseudo-first order rate constants of the 4-CP degradation by these materials under visible light illumination (b) ([2-EI-TiO$_2$] = 0.5 g/L, [4-CP]$_0$ = 10 μM, I = 6.43 × 10^{-6} Einstein/L·s (fluorescent lamp, λ > 400 nm))
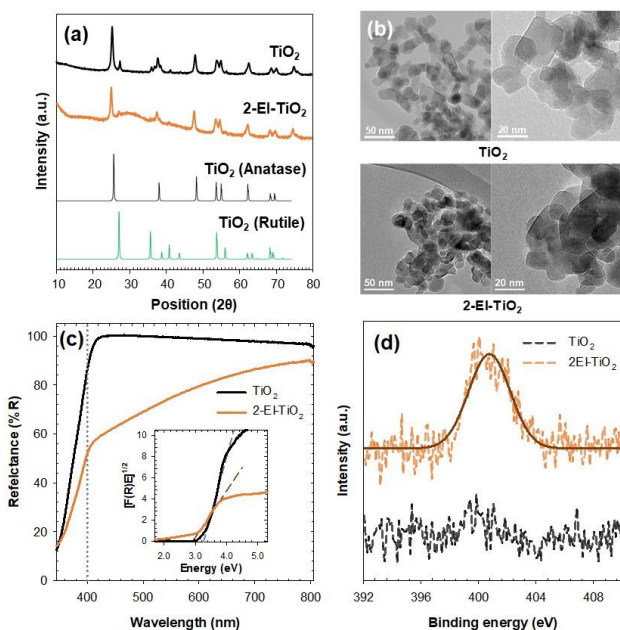

Fig. 2 X-ray diffraction patterns (a), TEM images (b), diffuse reflectance spectra (c), and X-ray photoelectron spectra (N 1s level) (d) of TiO$_2$ and 2-EI-TiO$_2$

The modified Kubelka-Munk function is given as $[F(R)E]^{\frac{1}{2}}$, where E indicates the light energy. The determined bandgap values of 2-EI-TiO$_2$ and TiO$_2$ were 2.92 eV and 3.27 eV, respectively.

The N 1s XPS spectrum of 2-EI-TiO$_2$ exhibited a broad peak at 400.5 eV, whereas that of bare TiO$_2$ did not display any characteristic peak (Fig. 2(d)). This confirms the nitrogen-doping on the surface of 2-EI-TiO$_2$. Typically, the N 1s peak is found at about 396 to 397 eV if the nitrogen atom is in the anionic state (e.g., N-Ti-N) (Asahi *et al*. 2001, Nasir *et al*. 2014). And it is found at about 397 to 400 eV if it is in the cationic state of Ti-O-N (Kim *et al*. 2014,

Nasir *et al*. 2014). Therefore, the N 1s peak of 2-EI-TiO$_2$ is found at 400.5 eV and indicates that the nitrogen atom is doped in the cationic state.

3.2 Photocatalytic degradation of organic compounds

The degradation of 4-CP by 2-EI-TiO$_2$, bare TiO$_2$, and bare TiO$_2$ plus 2-EI (a mixture of TiO$_2$ and 2-EI) was examined under visible light illumination (Fig. 3(a)). Bare TiO$_2$ and its mixture with 2-EI showed poor photocatalytic activity to degrade 4-CP; in 240 min 4-CP was degraded by 29% and 37%, respectively. The visible light-responsive activity of bare TiO$_2$ appears to result from the ligand-to-metal charge transfer pathway (Kim and Choi 2005). In contrast, 2-EI-TiO$_2$ degraded approximately 80% of 4-CP in 240 min under visible light illumination.

The photocatalytic degradation of different organic compounds (BA, phenol, 4-CP, AAP, and CBZ) was examined under visible light illumination (Fig. 3(b)). Phenol was degraded to a similar efficiency to 4-CP; the degradation of phenol was about 80% in 240 min. AAP was degraded even faster than phenol. However, BA and CBZ were resistant to the degradation by illuminated 2-EI-TiO$_2$; the degradation efficiencies of BA and CBZ in 240 min were only 16% and 24%, respectively.

To test the photochemical stability of 2-EI-TiO$_2$, the photocatalytic degradation of 4-CP by illuminated 2-EI-TiO$_2$ was repeated over 4 cycles (Fig. 4). For the first cycle, 1 μM 4-CP was degraded in the 2-EI-TiO$_2$ suspension for 60 min. Then, the concentration of 4-CP was adjusted to 1 μM at the beginning of each following cycle. The degradation efficiency of 4-CP gradually decreased over the 4 cycles (i.e., 99%, 83%, 78%, and 70% at each cycle). This indicates that the photocatalytic activity of 2-EI-TiO$_2$ decreases during the reaction. The accumulated degradation
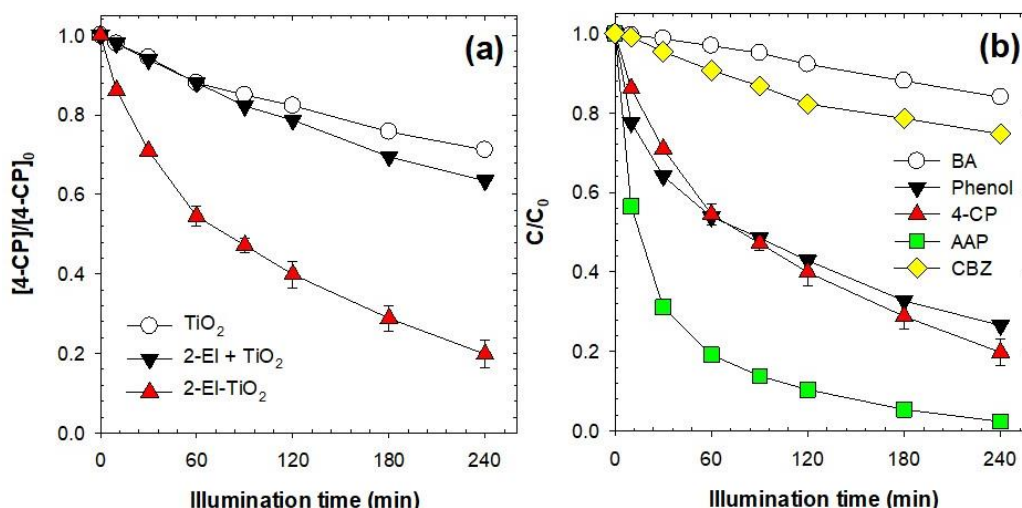
Fig. 3. Degradation of organic compounds by 2-EI-TiO₂ under visible light illumination: comparison of 4-CP degradation by 2-EI-TiO₂, bare TiO₂, and bare TiO₂ plus 2-EI (a) and degradation of different organic compounds (b) ([2-EI-TiO₂]₀ = 0.5 g/L, I = 6.43 × 10⁻⁶ Einstein/L·s (fluorescent lamp, λ > 400 nm), [4-CP]₀ = 10 μM for (a), [BA]₀ = [Phenol]₀ = [4-CP]₀ = [AAP]₀ = [CBZ]₀ = 10 μM for (b))

products may also inhibit the 4-CP degradation by scavenging reactive species.

3.3 The effects of ·OH scavengers and oxidant probes

The effects of $^{\bullet}$OH scavengers (methanol and *tert*-butanol) on the photocatalytic degradation of pollutants were examined (Fig. 5(a)). The target organic pollutant was MC-LR, a cyanobacterial toxin known to have acute hepatotoxicity. An excess amount of $^{\bullet}$OH scavengers (200 mM) was used to scavenge free and surface-bound $^{\bullet}$OH. It has been shown that *tert*-butanol scavenges free $^{\bullet}$OH, and methanol scavenges both free and surface-bound $^{\bullet}$OH (M. Cho *et al*. 2005). As shown in Fig. 5(a), the effects of methanol and *tert*-butanol were minor.

The oxidative transformation of the probe compounds (methanol and BA) was examined to evaluate the production of reactive oxidants by illuminated 2-EI-TiO₂ (Fig. 5(b)). An excess amount of methanol and BA was used to capture all reactive oxidants generated. The major oxidation products of methanol and BA were quantified, which are HCHO and *p*-HBA, respectively. The production of *p*-HBA from BA is indicative of the generation of $^{\bullet}$OH. As shown in Fig. 5(b), the concentration of HCHO increased up to 16.9 μM in 60 min. However, the production of *p*-HBA was negligible.

4. Discussion

4.1 Role of 2-EI

Several earlier studies have used 2-EI as a reducing agent to generate oxygen vacancies in TiO₂ (denoted as reduced TiO₂ in this study) (Zuo *et al*. 2010, Hamdy *et al*. 2012, Zou *et al*. 2013). In the sintering process, 2-EI

combusts to CO, CO₂, NO, and NO₂. The gases produced by incomplete combustion of 2-EI such as CO and NO react with oxygen atoms in the TiO₂ lattice, generating the oxygen vacancies.

In this study, 2-EI was mainly used as a nitrogen-doping agent; the sintering temperature in this study is lower than those in the previous studies. There is much evidence presented for the role of 2-EI as a nitrogen-doping agent rather than a reducing agent. First, the XRD spectrum of 2-EI-TiO₂ showed both the anatase and rutile phases (Fig. 2(a)). This contrasts the fact that the crystal phases of reduced TiO₂ were mostly rutile. It is known that the oxygen vacancies in reduced TiO₂ cause the phase transition from anatase to rutile phases in the sintering process (Zou *et al*. 2013). Second, the XPS spectrum of 2-EI-TiO₂ showed a broad N 1s peak at 400.5 eV (Fig. 2(d)), which is generally not found in the XPS spectrum of reduced TiO₂.

4.2 Mechanism of organic compound degradation by illuminated 2-EI-TiO₂

Light-illuminated TiO₂ generates reactive redox species on the surface. The light illumination onto the TiO₂ surface generates electron-hole pairs, which further produce reactive oxygen species as $^{\bullet}$OH and superoxide radical anion ($O_2^{\bullet-}$) by redox reactions of water and molecular oxygen. Among the photogenerated reactive species, $^{\bullet}$OH and holes are usually responsible for the degradation of organic compounds.

The experimental results of this study suggest that 2-EI-TiO₂ does not significantly generate $^{\bullet}$OH. $^{\bullet}$OH ($E^{\circ}[^{\bullet}OH/H_2O] = +2.80$ V$_{NHE}$) as a strong oxidant nonselectively reacts with organic compounds at diffusion-controlled rates; the second order rate constants for the $^{\bullet}$OH reactions are higher than 10^9 M⁻¹ s⁻¹ for most of organic compounds including those used in this study (Buxton *et al*. 1988). However, the degradation of organic compounds by
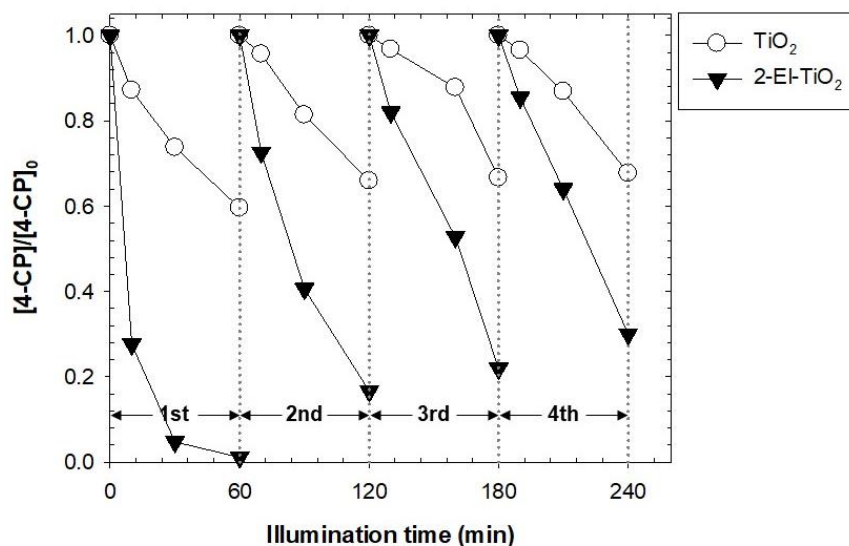
Fig. 4. Repeated degradation of 4-CP by 2-EI-TiO$_2$ under visible light illumination ([2-EI-TiO$_2$]$_0$ = 0.5 g/L, [4-CP]$_0$ = 1 μM, I = 6.43 × 10^{-6} Einstein/L·s (fluorescent lamp, λ > 400 nm))
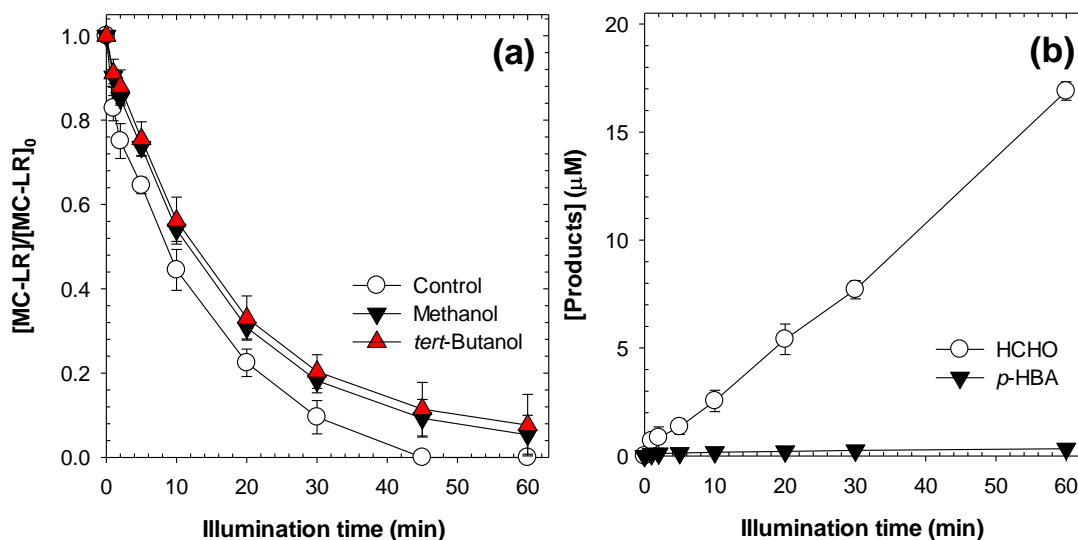

Fig. 5. Effects of ·OH scavengers (a), and production of HCHO and p–HBA (b) by 2-EI-TiO$_2$ under visible light illumination ([2-EI-TiO$_2$]$_0$ = 0.5 g/L, I = 2.46 × 10^{-5} Einstein/L·s (Xenon arc lamp, λ > 400 nm), [MC-LR]$_0$= 0.1 μM for (a), [Methanol]$_0$ = [*tert*-Butanol]$_0$ = 200 mM for (a), [Methanol]$_0$ = 200 mM for (b), [BA]$_0$ = 10 mM for (b))

illuminated 2-EI-TiO$_2$ was selective (Fig. 3(b)). This is inconsistent with the behaviors of ·OH reactions. Second, the minor effects of ·OH scavengers indicate that ·OH is not responsible for the degradation of 4-CP (Fig. 5(a)). Also, the negligible production of *p*-HBA from BA supports the observation of insignificant generation of ·OH (Fig. 5(b)).

The oxidation by photogenerated holes appears to be mainly responsible for the degradation of organic compounds by illuminated 2-EI-TiO$_2$. The nitrogen-doping creates a mid-gap band above the valence band of TiO$_2$ (Zhang *et al.* 2010, Kim *et al.* 2014). It narrows the bandgap so that TiO$_2$ can utilize visible light. However, the oxidizing power of the valence band holes decreases. Therefore, the generated holes fail to oxidize water into ·OH, and selectively oxidize organic compounds. The weak oxidizing power of 2-EI-TiO$_2$ may cause the accumulation

of oxidation products, decreasing the photochemical reactivity of 2-EI-TiO$_2$.

5. Conclusions

In this study, 2-EI-TiO$_2$ was synthesized by a simple modification of commercial TiO$_2$ using 2-EI as a nitrogen-doping agent. 2-EI-TiO$_2$ showed similar crystallinity and morphology comparing to bare TiO$_2$. However, 2-EI-TiO$_2$ showed effective visible light absorption due to the narrowed bandgap. The XPS spectrum confirmed the doping of cationic nitrogen on the surface of 2-EI-TiO$_2$. The visible light-illuminated 2-EI-TiO$_2$ that selectively degraded organic compounds. In the photocatalytic degradation of organic compounds by illuminated 2-EI-TiO$_2$, the role of

•OH can be excluded. The oxidation by photogenerated holes appear to be mainly responsible for the degradation of organic compounds.

Acknowledgements

References

Asahi, R., Morikawa, T., Ohwaki, T., Aoki, K. and Taga, Y. (2001), "Visible-light photocatalysis in nitrogen-doped titanium oxides", *Science*, **293**(5528), 269-271.

Buxton, G.V., Greenstock, C.L., Helman, W.P. and Ross, A.B. (1988), "Critical review of rate constants for reactions of hydrated electrons, hydrogen atoms and hydroxyl radicals (•OH/•O$^-$) in aqueous solution", *J. Phys. Chem. Ref. Data*, **17**(2), 513-886.

Devi, L.G., Nagaraj, B. and Rajashekhar, K.E. (2012), "Synergistic effect of Ag deposition and nitrogen doping in TiO$_2$ for the degradation of phenol under solar irradiation in presence of electron acceptor", *Chem. Eng. J.*, **181-182**, 259-266.

Fujishima, A., Rao, T.N. and Tryk, D.A. (2000), "Titanium dioxide photocatalysis", *J. Photochem. Photobiol. C-Photochem. Rev.*, **1**(1), 1-21.

Gole, J.L., Stout, J.D., Burda, C., Lou, Y. and Chen, X. (2004), "Highly efficient formation of visible light tunable TiO$_{2-x}$N$_x$ photocatalysts and their transformation at the nanoscale", *J. Phys. Chem. B*, **108**(4), 1230-1240.

Hamdy, M.S., Amrollahi, R. and Mul, G. (2012), "Surface Ti^{3+}-containing (blue) titania: A unique photocatalyst with high activity and selectivity in visible light-stimulated selective oxidation", *ACS Catal.*, **2**(12), 2641-2647.

Hanaor, D.A.H. and Sorrell, C.C. (2011), "Review of the anatase to rutile phase transformation", *J. Mater. Sci.*, **46**(4), 855-874.

He, T., Guo, X., Zhang, K., Feng, Y. and Wang, X. (2013), "Synthesis and characterization of B-N co-doped mesoporous TiO$_2$ with enhanced photocatalytic activity", *RSC Adv.*, **4**, 5880-5886.

Hoffmann, M.R., Martin, S.T., Choi, W. and Bahnemann, D.W. (1995), "Environmental applications of semiconductor photocatalysis", *Chem. Rev.*, **95**(1), 69-96.

In, S., Orlov, A., Berg, R., Garcia, F., Pedrosa-Jimenez, S., Tikhov, M.S., Wright, D.S. and Lambert, R.M. (2007), "Effective visible light-activated B-doped and B,N-codoped TiO$_2$ photocatalysts", *J. Am. Chem. Soc.*, **129**(45), 13790-13791.

Kang, M. (2005), "The superhydrophilicity of Al-TiO$_2$ nanometer sized material synthesized using a solvothermal method", *Mater. Lett.*, **59**(24-25), 3122-3127.

Kim, S. and Choi, W. (2005) "Visible-light-induced photocatalytic degradation of 4-chlorophenol and phenolic compounds in aqueous suspension of pure titania: Demonstrating the existence of a surface-complex-mediated path" *J. Phys. Chem. B,* **109**(11), 5143-5149.

Kim, S., Hwang, S.J. and Choi, W. (2005), "Visible light active platinum-ion-doped TiO$_2$ photocatalyst", *J. Phys. Chem. B*, **109**(51), 24260-24267.

Kim, W., Tachikawa, T., Kim, H., Lakshminarasimhan, N.,

Murugan, P., Park, H., Majima, T. and Choi, W. (2014), "Visible light photocatalytic activities of nitrogen and platinum-doped TiO$_2$: Synergistic effects of co-dopants", *Appl. Catal. B-Environ.*, **147**, 642-650.

Nasir, M., Bagwasi, S. Jiao, Y., Chen, F., Tian, B. and Zhang, J. (2014), "Characterization and activity of the Ce and N co-doped TiO$_2$ prepared through hydrothermal method", *Chem. Eng. J.*, **236**, 388-397.

Neville, E.M., MacElroy, J.M.D., Thampi, K.R. and Sullivan J.A. (2013), "Visible light active C-doped titanate nanotubes prepared via alkaline hydrothermal treatment of C-doped nanoparticulate TiO$_2$: Photo-electrochemical and photocatalytic properties", *J. Photochem. Photobiol. A-Chem.*, **267**, 17-24.

Park, H., Park, Y., Kim, W. and Choi, W. (2013), "Surface modification of TiO$_2$ photocatalyst for environmental applications", *J. Photochem. Photobiol. C-Photochem. Rev.*, **15**, 1-20.

Pelaez, M., Nolan, N.T., Pillai, S.C., Seery, M.K., Falaras, P., Kontos, A.G., Dunlop, P.S.M., Hamilton, J.W.J., Byrne, J.A., O'Shea, K., Entezari, M.H. and Dionysiou, D.D. (2012), "A review on the visible light active titanium dioxide photocatalysts for environmental applications", *Appl. Catal. B-Environ.*, **125**, 331-349.

Periyat, P., Pillai, S.C., McCormack, D.E., Colreavy, J. and Hinder, S.J. (2008), "Improved high-temperature stability and sun-light-driven photocatalytic activity of sulfur-doped anatase TiO$_2$", *J. Phys. Chem. C*, **112**(20), 7644-7652.

Ruqaishy, M.A., Marzouqi, F.A., Qi, K., Liu, S.Y., Karthikeyan, S., Kim, Y., Al-Kindy, S.M.Z., Kuvarega, A.T. and Selvaraj, R. (2018), "Template-free preparation of TiO$_2$ microspheres for the photocatalytic degradation of organic dyes", *Korean J. Chem. Eng.*, **35**(11), 2283-2289.

Sakthivel, S. and Kisch, H. (2003), "Daylight photocatalysis by carbon-modified titanium dioxide", *Angew. Chem. Int. Edit.*, **42**(40), 4908-4911.

Sathish, M., Viswanathan, B. and Viswanath, R.P. (2007), "Characterization and photocatalytic activity of N-doped TiO$_2$ prepared by thermal decomposition of Ti-melamine complex", *Appl. Catal. B-Environ.*, **74**(3-4), 307-312.

Schneider, J., Matsuoka, M., Takeuchi, M., Zhang, J., Horiuchi, Y., Anpo, M. and Bahnemann, D.W. (2014), "Understanding TiO$_2$ photocatalysis: Mechanisms and materials", *Chem. Rev.*, **114**(19), 9919-9986.

Selvam, K. and Swaminathan, M. (2012), "Nano N-TiO$_2$ mediated selective photocatalytic synthesis of quinaldines from nitrobenzenes", *RSC Adv.*, **2**(7), 2848-2855.

Vinu, R. and Madras, G. (2008), "Kinetics of simultaneous photocatalytic degradation of phenolic compounds and reduction of metal ions with nano-TiO$_2$", *Environ. Sci. Technol.*, **42**(3), 913-919.

Wang, S.Q., Liu, W.B, Fu, P. and Cheng, W.L. (2017), "Enhanced photoactivity of N-doped TiO$_2$ for Cr(VI) removal: Influencing factors and mechanism", *Korean J. Chem. Eng.*, **34**(5), 1584-1590.

Yuan, R., Liu, D., Wang, S., Zou, B. and Ma, F. (2018) "Enhanced photocatalytic oxidation of humic acids using Fe^{3+}-Zn^{2+} co-doped TiO$_2$: The effects of ions in aqueous solutions*, Environ. Eng. Res.*, **23**(2), 181-188.

Yu, J.C., Ho, W., Yu, J., Yip, H., Wong, P.K. and Zhao, J. (2005), "Efficient visible-light-induced photocatalytic disinfection on sulfur-doped nanocrystalline titania", *Environ. Sci. Technol.*, **39**(4), 1175-1179.

Zhang, J., Wu, Y., Xing, M., Leghari, S.A.K. and Sajjad, S. (2010), "Development of modified N doped TiO$_2$ photocatalyst with metals, nonmetals and metal oxides", *Ener. Environ. Sci.*, **3**, 715-726.

Zou, X., Liu, J., Su, J., Zuo, F., Chen, J. and Feng, P. (2013),

"Facile synthesis of thermal- and photostable titania with paramagnetic oxygen vacancies for visible-light photocatalysis", *Chem. Eur. J.*, **19**(8), 2866-2873.

Zuo, F., Wang, L., Wu, T., Zhang, Z., Borchardt, D. and Feng, P. (2010), "Self-doped Ti^{3+} enhanced photocatalyst for hydrogen production under visible light", *J. Am. Chem. Soc.*, **132**(34), 11856-11857.

CC